

Luiz A. Colnago<sup>1</sup>  
Fabiana D. Andrade<sup>2</sup>  
André A. Souza<sup>3</sup>  
Rodrigo B. V. Azeredo<sup>4</sup>  
Allan A. Lima<sup>5</sup>  
Lucas M. Cerioni<sup>6</sup>  
Tristán M. Osán<sup>7</sup>  
Daniel J. Pusiol<sup>8</sup>

<sup>1</sup> Embrapa Instrumentação,  
São Carlos, SP, Brazil.

<sup>2</sup> Instituto de Química de São  
Carlos, São Carlos, SP, Brazil.

<sup>3</sup> Schlumberger Brazil Research  
and Geoenvironment Center,  
Rio de Janeiro, RJ, Brazil.

<sup>4</sup> Universidade Federal  
Fluminense, Instituto de  
Química, Niterói, RJ, Brazil.

<sup>5</sup> Departamento de Engenharia  
Elétrica e Computação, Escola  
de Engenharia de São Carlos,  
São Carlos, SP, Brazil.

<sup>6</sup> Spinlock S.R.L., Consejo  
Nacional de Investigaciones  
Científicas y Técnicas  
(CONICET), Córdoba,  
Argentina.

<sup>7</sup> Consejo Nacional de  
Investigaciones Científicas y  
Técnicas (CONICET), Facultad  
de Matemática, Astronomía y  
Física, Universidad Nacional  
de Córdoba, Córdoba,  
Argentina.

<sup>8</sup> Consejo Nacional de  
Investigaciones Científicas y  
Técnicas (CONICET), Instituto  
de Física Enrique Gaviola  
(IFEG), Córdoba, Argentina.

**Correspondence:** Dr. Luiz A. Colnago (luiz.colnago@embrapa.br),  
Embrapa Instrumentação, Rua XV de Novembro 1452, São Carlos, SP,  
13560-970, Brazil.

## Review

# Why is Inline NMR Rarely Used as Industrial Sensor? Challenges and Opportunities

Although nuclear magnetic resonance (NMR) is one of the most powerful analytical techniques, it has not been widely used as a non-destructive, non-contact inline industrial sensor. A short background of NMR spectroscopy fundamentals and instrumentation is presented along with its potential applications and limitations for real-time analysis in the manufacturing sector. NMR signals are generated in the presence of a magnetic field normally produced by expensive large and heavy magnets which have been the major limiting factor in the use of NMR analysis in factories. However, the last decade has brought substantial advances in the development of cheaper, smaller, and lighter permanent magnets based on rare earth materials that use Halbach and unilateral configurations. Small and light cryogenic-free superconducting magnets are now offered in the market and are opening a new era in manufacturing. It is expected that soon NMR spectroscopy will be applied to monitor the chemical and physical properties of complex feedstock mixtures and reactions in real time which is the ultimate goal of precise process control.

**Keywords:** Industrial sensor, Inline analysis, NMR, Process control

*Received:* June 06, 2013; *revised:* September 09, 2013; *accepted:* October 29, 2013

**DOI:** 10.1002/ceat.201300380

## 1 Introduction

Since the detection of the nuclear magnetic resonance (NMR) phenomenon in 1946 by two independent groups of physicists, NMR has fascinated the scientific community with its new and revolutionary application [1–4]. Less than ten years after its discovery, the first commercial continuous-wave <sup>1</sup>H high-resolution NMR spectrometer (HR-NMR) was offered on the market. This technique was a giant leap towards determining the structure of organic molecules and reduced the structure elucidation times from months/years to days/weeks. In the late 1960s, commercial pulsed and Fourier transform NMR spectrometers (FT-NMR) and high-field superconductor magnets were introduced to detect nuclei, such as <sup>13</sup>C, for which this technique has low sensitivity [1–3]. Two new developments were introduced in the early 1970s: multidimensional NMR and magnetic resonance imaging (MRI). Multidimensional NMR revolutionized the determination of 3D structures of proteins in solution, opening a new era to the pharmaceutical industry. Furthermore, MRI is currently one of the most important medical diagnostic tools. Several of these discoveries and implementations received the Nobel Prize in subsequent years. Felix Bloch and Edward Mills Purcell were recognized for their work in physics in 1952, Richard Ernst's work on FT and multidimensional NMR received the prize in chemistry in 1991, Kurt Wüthrich in chemistry in 2002 for describing the

protein structure by multidimensional NMR, and Paul Lauterbur and Peter Mansfield in 2003 for the introduction of MRI.

Despite these contributions, NMR also has many other very important applications in polymers, ceramics, cement, inorganic chemistry, natural products, food, in vivo chemical analysis, metabolomics, oil well-logging, and process analysis, just to name a few. Therefore, NMR is currently used in almost all scientific fields to obtain chemically, biologically, and/or physically relevant information.

Even though NMR has such a strong analytical potential, it has not been widely used as a non-destructive, non-contact, inline industrial sensor. This disparity is surprising because almost every other type of physical methods, such as infrared (NIR, FTIR, Raman) or UV-VIS spectroscopies, ultrasound velocity or attenuation measurements, have been employed as an online instrumentation in the industrial sector, even though these methods are less selective and have fewer applications [5–9]. Thus, this paper presents a short description of the fundamentals and instrumentation of NMR spectroscopy, its potential applications and limitations for real-time analysis in the industrial sector, as well as a discussion of associated challenges and opportunities.

## 2 NMR Spectroscopy

To understand potential applications and limitations of NMR as an industrial sensor, it is necessary to discuss some of the basic principles of NMR spectroscopy and instrumentation and compare this method with other physical methods. Detailed information on NMR spectroscopy is available in several textbooks [1–4].

NMR is a spectroscopic technique to observe nuclear spin transitions when the sample is placed in a static magnetic field with a magnetic flux density ( $B_0$ ) in Tesla (T) and irradiated with an oscillating magnetic field ( $B_1$ ), with an angular frequency (Eq. (1)):

$$\omega = \gamma B_0 \quad (1)$$

where  $\gamma$  is the magnetogyric ratio which is a constant for each isotope.

Considering this relation, the advantages and disadvantages of NMR will be discussed with respect to  $\gamma$ , related to the sample, the transmitted/received radiofrequency ( $\nu = \omega/2\pi$ ) and  $B_0$  which are instrumental factors. The different methods to detect NMR signals and to enhance the signal-to-noise ratio (S/N), and to reduce the analytical time will also be discussed.

### 2.1 Sample Requirements

NMR is applied to analyze samples containing nuclei possessing a magnetic moment ( $\mu$ ) and angular momentum or spin ( $S$ ). These properties are closely related by  $\mu = \gamma S$ . As the nuclear spin is an isotope-specific property related to the particular element and nuclide, NMR and chemistry are closely connected because almost all elements have at least one isotope with nuclear spin [10]. Nuclear spin is observed in isotopes

with odd numbers of protons and/or neutrons. Consequently, it is not observed in isotopes with an even atomic number ( $Z$ ) and even mass number ( $A$ ). For example, the three hydrogen isotopes  $^1\text{H}$  (hydrogen),  $^2\text{H}$  (deuterium), and  $^3\text{H}$  (tritium) can be detected by NMR. Conversely, other important elements, such as carbon, oxygen, and sulfur, can only be observed by their naturally rare isotopes  $^{13}\text{C}$ ,  $^{17}\text{O}$ , and  $^{33}\text{S}$  because their common forms do not have spin. Tab. 1 presents the  $\gamma$ -values, natural abundance, and relative sensitivity to  $^1\text{H}$ . This table indicates that NMR is most sensitive for  $^1\text{H}$  and  $^{19}\text{F}$  and less sensitive for the  $^{31}\text{P}$  and  $^{13}\text{C}$  isotopes by one and two orders of magnitude compared to  $^1\text{H}$ . Fortunately, most industrial products contain  $^1\text{H}$  that has two important properties for NMR observation, namely, high  $\gamma$ -value and high natural abundance.

**Table 1.** Magnetogyric ratio, natural abundance, and relative sensitivity to  $^1\text{H}$  (100%), for some of the NMR-sensitive isotopes.

Nucleus	$\gamma$ [ $10^7 \text{ rad T}^{-1} \text{ s}^{-1}$ ]	Natural abundance [%]	Relative sensitivity [%]
$^1\text{H}$	26.75	99.98	100.0
$^{19}\text{F}$	25.18	100.00	83.3
$^{31}\text{P}$	10.84	100.00	6.6
$^{13}\text{C}$	6.73	1.07	1.6

### 2.2 Static Magnetic Field

NMR transitions are observed only when the samples are in the presence of a magnetic field ( $B_0$ ) used to split the nuclear energy levels (Zeeman splitting) [1–4]. The necessity of this magnetic field is the major difference between NMR and other spectroscopy techniques used as industrial sensors. It is also the major limiting factor for industrial sensors, as discussed below.

The magnetic field breaks the degeneracy, i.e., it splits the spins ( $S$ ) into  $2S + 1$  energy levels. For  $S = 1/2$ , ( $^1\text{H}$ ,  $^{13}\text{C}$ ,  $^{19}\text{F}$ ), there are two energy states,  $\alpha$  and  $\beta$ , equivalent to the parallel and anti-parallel orientation to  $B_0$  with an energy difference of  $\Delta E = h\nu$  where  $h$  is Planck's constant and  $\nu$  denotes excitation frequency (Hz). The energy difference can also be written as  $\Delta E = h\nu = (\gamma B_0/2\pi)$ .

The spin population at each energy level depends on  $B_0$ ,  $\gamma$ ,  $k$ , and the temperature according to the Boltzmann equation (2):

$$N_\beta/N_\alpha = e^{-\Delta E/kT} = e^{-(h\gamma B_0/2\pi)/kT} \quad (2)$$

where  $N_\alpha$  represents the population at the lower energy level,  $N_\beta$  the population at the higher energy level,  $k$  is the Boltzmann constant, and  $T$  is the temperature (in Kelvin).

This equation demonstrates that there is a small excess of population at the lower energy state  $\alpha$  (e.g., 1 part in  $10^5$  spins for a  $B_0$  of about 1 T) at room temperature [1]. This very small difference in populations gives rise to a net magnetization  $M_0$ .

$M_0$  is the sum of the magnetic momenta,  $\Sigma\mu$ , of the excess of spins populating the low energy level,  $M_0 = \Sigma\mu$ .

The polarization process is not instantaneous and the magnetization increases exponentially with a time constant  $T_1$ , according to Eq. (3) [1]:

$$M_z(\tau) = M_0(1 - e^{-\tau/T_1}) \quad (3)$$

where  $M_z$  represents the component of the magnetization along the direction of  $B_0$ ,  $M_0$  the magnetization of the thermal equilibrium,  $T_1$  the longitudinal relaxation time, and  $\tau$  a time interval.

$T_1$  is a very important property that must be taken into account in all quantitative NMR measurements [1–9]. Furthermore, this constant is crucial in flow measurements (continuous or stop-and-flow) because the sample needs to travel a distance ( $d$ ) equal  $5T_1$  times the flow velocity ( $v$ ), i.e.,  $d = 5T_1v$ , in the magnetic field before the analysis, in order to reach 99.33 % of the magnetization of the thermal equilibrium ( $M_0$ ) [1, 5–11].

Accordingly,  $M_0$  is related to the sensitivity (intensity) of the NMR signal and depends on the magnetic field ( $B_0$ ), number of spins ( $N$ ), magnetogyric ratio ( $\gamma$ ), spin ( $S$ ), Boltzmann constant ( $k$ ), and temperature ( $T$ ), as indicated in Eq. (4). Approximately  $10^{14}$  spins are necessary for an NMR experiment to produce a good signal-to-noise ratio in the spectrum [1]. This requirement necessitates a large amount of sample when compared with other higher energy spectroscopy methods, such as UV spectroscopy.

$$M_0 = N\gamma^2(h/2\pi)^2 B_0 S(S+1)/3kT \quad (4)$$

According to the classical model, in the absence of  $B_0$ , the orientation of the nuclear magnetic moment ( $\mu$ ) is isotropic. When exposed to  $B_0$ , the  $\mu$  vector starts to precess about the direction of  $B_0$  (the  $z$ -direction), with an angular frequency  $\omega$  known as the Larmor frequency (Eq. (1)). Besides,  $B_0$  influences the spectral resolution because even the magnetic field produced by the best magnets is not perfectly homogeneous. Since the Larmor frequency varies with the magnetic field, the spectral line width depends on the magnetic field inhomogeneity  $\Delta B_0$ . Consequently, to improve the resolution, the homogeneity of  $B_0$  needs to be optimized by shimming procedures [1–4].

For low-resolution NMR, passive shimming performed with mechanical adjustments or the addition of metallic or magnetic pieces is sufficient. However, medium- and high-resolution applications require additional active shimming procedures that use coils and adjustable currents. Passive shimming is normally performed in the magnet assembly, whereas active shimming must be carried out for every sample or on a daily basis for high- and medium-resolution scans. Furthermore,  $B_0$  influences the resolution due to the most important selective parameter in HR-NMR, the chemical shift, which linearly depends on the magnetic field strength [1–4].

Hence, the need of a magnetic field is one of the major disadvantages of NMR when compared with other physical methods [5–9, 11, 12]. The magnet increases the cost of the

instrument because it can represent up to a half of its price. The magnet also limits the applications because it normally is a bulky and heavy component that needs to be in close proximity to the analyte. The magnet may also be affected by the movement of large metallic objects, such as vehicles or elevators, and it may attract small magnetic parts such as bolts, nuts, or metallic fragments common in industrial environments. It may also magnetize components around it, or at worst, harm unaware people.

### 2.3 NMR Excitation and Detection

To obtain the NMR signal, the sample in the magnetic field is irradiated with an oscillating magnetic field ( $B_1$ ) with an angular frequency  $\omega = 2\pi\nu$ .  $B_1$  is produced when a radio frequency (rf) is applied to an NMR probe (antenna). When the condition set by Eq. (1) is reached, the sample absorbs energy and the NMR signal can be detected.

Although the NMR signal is much weaker than that obtained by other physical methods, the use of radio frequency technology has several advantages over the excitation and detection of the other physical methods. Radiofrequency (rf) signals can be generated with high precision and yield high-resolution measurements as compared with other spectroscopic methods, which normally use a polychromatic source that has to be filtered in order to obtain a monochromatic frequency with a very broad line width or low resolution [1].

NMR signals can be excited and detected in several ways. The most popular methods are known as continuous-wave (CW) and pulsed NMR [1–4]. The CW-NMR spectrometers were mostly employed from the infancy of NMR spectroscopy up to the 1970s. CW spectrometers normally use low-power and fixed rf and sweep the  $B_0$  to meet the resonance condition for each NMR signal. The sweeping time depends on the adiabatic condition which leads to a very long scanning time (tens of minutes) for HR-NMR. This long scanning time is the major disadvantage of the CW method as compared with pulsed NMR (measurements on the order of a few seconds).

For low-resolution spectra, the sweep can be performed much faster. Nevertheless, very broad lines (solid or high-viscosity solutions) are complicated to detect by a reduction in signal intensity, since the integrated signal intensity is proportional to the sample concentration. When solid and liquid components are present at similar concentrations in heterogeneous samples, the solid signal is in the baseline or at noise level, even when the liquid signal has a very high signal-to-noise ratio. Consequently, the solid content is hard to detect.

Although a rapid CW scan method [13] has been proposed to accelerate high-resolution analysis, it has not been widely adopted because the acquired spectrum cannot be directly analyzed due to the need for a computer to obtain a useful spectrum. In addition, the introduction of pulsed and FT-NMR improved the speed of data acquisition over the rapid CW scan method. Since the pulsed spectrometer is the current standard method to obtain NMR signals [1–4], this method will be discussed in more detail.

## 2.4 Pulsed NMR

In a pulsed NMR spectrometer, the transmitter produces very short and intense rf pulses to excite all frequencies in the NMR spectrum. During the rf pulse, the magnetization is rotated by an angle  $\theta$ , defined by Eq. (5):

$$\theta = \gamma B_1 t_p \quad (5)$$

where  $\theta$  is the flip angle, i.e., the angle between the magnetization vector and  $z$ -axis, and  $t_p$  is the duration of the rf pulse.

To obtain the maximum signal ( $\theta = 90^\circ$ ) in a few microseconds, the pulsed  $B_1$  must be several orders of magnitude stronger than the one used in CW experiments.  $B_1$  depends on the rf power ( $P$ ), the resonance frequency in MHz ( $\nu$ ), and the volume ( $V$ ) and quality factor ( $Q$ ) of the probe coil (Eq. (6)) [4]. For a specific resonance frequency and probe, the  $B_1$  value is adjusted by the transmitter rf power that may vary from tens to thousands of watts, in order to obtain the flip angle in few microseconds.

$$B_1 \sim 3(PQ/\nu V)^{\frac{1}{2}} \quad (6)$$

After the pulse, the magnetization precesses again around  $B_0$ , inducing an NMR signal in the probe coil. This signal is named free induction decay (FID). After the pulse, the NMR signal relaxes by two distinct relaxation processes ruled by the longitudinal ( $T_1$ ) and transverse relaxation ( $T_2$ ) times.

### 2.4.1 Longitudinal Relaxation

The longitudinal relaxation is an exponential process with a time constant  $T_1$  (Eq. (3)) that is involved in returning the magnetization to the thermal equilibrium along the  $z$ -axis ( $z$ -axis is parallel to  $B_0$ ). Because this process involves energy transfer to the surrounding environment (lattice), it is also known as spin-lattice relaxation. This process is identical to the process involved in the magnetization buildup, after inserting the sample in the magnetic field. Thus, without knowledge of  $T_1$  and correcting for it, the recycling time between the pulse sequences must be at least  $5T_1$  for quantitative NMR measurements, since this amount of time is needed for the magnetization along the direction of  $B_0$  ( $M_z$ ) to reach approximately 99.33% of the thermal equilibrium magnetization ( $M_0$ ).

### 2.4.2 Transversal Relaxation

Although the transverse relaxation does not depend on energy transfer from the spins to the lattice like in the longitudinal relaxation process, it interferes with the decay of the NMR signal through the loss of magnetization coherence in the  $xy$  plane (the transverse plane to  $B_0$  direction). Since this loss is caused by the interaction among spins, it is also known as spin-spin relaxation.

Transverse relaxation causes an exponential decay of the  $M_{xy}$  signal with a time constant  $T_2$  (Eq. (7)):

$$M_{xy}(\tau) = M_{xy} e^{(-\tau/T_2)} \quad (7)$$

where  $T_2$  is the transverse relaxation time,  $M_{xy}$  represents the component of the magnetization on the  $xy$ -plane, and  $\tau$  is a time interval.

Both relaxation times depend on molecular mobility [1, 4]. Normally,  $T_1$  is long for liquid and solid samples, and minimized when the molecular dynamics approximate the resonance frequency.  $T_2$  approximates  $T_1$  for low-viscosity liquid samples, and its values decay to a minimum in solid samples ( $T_2 \ll T_1$ ).

Accordingly, the FID decay in a perfectly homogeneous magnet depends on  $T_2$ . However, the real  $B_0$  is not perfectly homogenous;  $\Delta B_0$  quickly disperses the magnetization in the  $xy$ -plane, sometimes much faster than  $T_2$ , particularly for liquid samples. Thus, the FID signal does not decay with  $T_2$  but with an effective transverse relaxation time  $T_2^*$ , given by Eq. (8) [4]:

$$1/T_2^* = 1/T_2 + \gamma \Delta B_0/2 \quad (8)$$

A faster decay in the time domain is equivalent to a broader line in the frequency domain. Thus, the NMR line width is  $\Delta\nu = 1/\pi T_2^*$ . Consequently, the shimming procedure is very important in HR-NMR to obtain the maximum resolution, i.e., the minimum  $\Delta B_0$  [1–4].

Despite the numerous advantages of pulsed NMR over CW, it cannot generate complete NMR data. In pulsed NMR, the data acquisition (FID) begins only after the instrumental dead time, a period when the receiver is overloaded by pulse leak, probe ringing, and other instrumental imperfections (Fig. 1). The dead time normally varies from few to hundreds of microseconds after the pulse and is an important instrumental char-

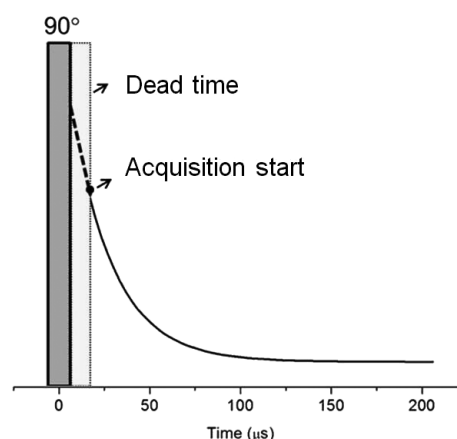


**Figure 1.** Time evolution of an NMR signal (FID) after a pulse. The dead time in this figure is approximately  $15 \mu\text{s}$ . The acquisition may start from this time and the FID decay with time constant  $T_2^*$ .

acteristic. In liquid materials or solutions with long  $T_2$ , the dead time is not a limiting factor. However, the dead time limits the detection of a solid material FID signal because the short  $T_2$  (on the order of few microseconds). The FID signal of solid samples may be at the noise level after the dead time, even in a very homogeneous magnet.

The FID amplitude after the dead time, which does not contain the solid component signals, has been widely used in off-line industrial applications of low-resolution NMR to quantify the liquid components ( $T_2$  on the order of several hundreds of milliseconds), of homogeneous and heterogeneous samples [5–9]. The FID signal has been employed to measure the total content of hydrogen in fuels, oil/fat or moisture in heterogeneous agriculture and food products, and total fluorite in toothpaste [14–19].

The FID signal cannot be taken to measure two or more components with long relaxation times (e.g., two liquid components) in low-resolution spectrometers due to the shorter  $T_2^*$ .

Pulse sequences to enhance the contrast between  $T_1$  and/or  $T_2$  are used to discriminate sample components with long and similar relaxation times [5–9]. The contrast between the components may be obtained by the difference in  $T_1$  by, e.g., the inversion recovery (IR) pulse sequence ( $180^\circ\text{-}\tau\text{-}90^\circ$ ) [1]. Similarly, to obtain the contrast between the  $T_2$  relaxation times, the spin-echo sequence (Fig. 2) [1] can be performed. In the *spin-echo* sequence ( $90^\circ\text{-}\tau\text{-}180^\circ$ ), the  $90^\circ$  pulse produces an FID (solid line) that contains the signal of the components with short and long  $T_2$ . This FID decays over a time  $\tau$  with a time constant  $T_2^*$ . The dotted lines represent the signal components of the spins with short and long  $T_2$  values, denoted as  $T_2(s)$  and  $T_2(l)$ , respectively. The  $180^\circ$  pulse creates a signal in the form of a spin-echo which is composed mainly of the  $T_2(l)$  at time  $2\tau$  [1, 6–9]. The echo amplitude depends on  $T_2$  but not on  $\Delta B_0$ . Therefore, a time  $\tau$  might be chosen to obtain an echo signal proportional to the concentration of the component with  $T_2(l)$ . This sequence was applied to quantify the solid/liquid ratio in fats and oil/moisture content in several agriculture and food products [14–24]. For more information about other low-field NMR applications see reviews [6, 8, 9, 25].

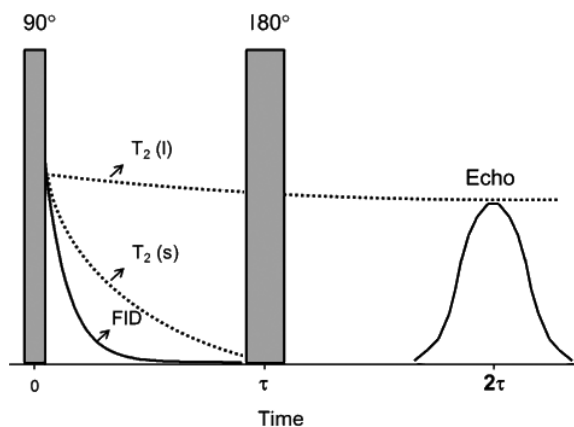


**Figure 2.** Diagram of the spin-echo sequence, with the FID signal (solid line) after the  $90^\circ$  pulse, the refocused  $180^\circ$  pulse after time  $\tau$  which produces an echo signal at  $2\tau$  of the first pulse. Dotted lines: decays for short (s) and long (l)  $T_2$  values.

The spin-echo sequence is also sensitive to molecular diffusion when the measurement is performed in an inhomogeneous magnetic field. Thus, the difference in molecular diffusion between large and small molecules might be used to discriminate these compounds by spin-echo or more sophisticated echo sequences with pulsed-field gradients (PFG) [5–8].

Even though most common NMR methods are based on FID and/or spin-echo intensity [14–19], other more sophisticated pulse sequences have been used in quantitative and qualitative low-resolution NMR analyses. The most popular of these sequences is the Carr-Purcell-Meiboom-Gill (CPMG) sequence [6–9, 23, 24, 26, 27]. This sequence consists of a train of  $180^\circ$  pulses separated by a time interval  $2\tau$  [4], which are preceded by a  $90^\circ$  pulse with a phase shift of  $90^\circ$  and a time interval  $\tau$  [1]. This sequence produces a series of echo signals, in a single scan, with decaying amplitudes modulated by  $T_2$ . The decay of the CPMG signal has been analyzed by mono- and multi-exponential fitting or inverse Laplace transform to obtain  $T_2$  values, or by multivariate methods to extract qualitative and quantitative information [4–6, 23, 26, 27]. The CPMG sequence has been used to measure the qualitative and quantitative properties of agriculture, food, and fuel products [5–9, 20–24, 26, 27].

Inversion recovery and other sequences to measure  $T_1$  have been barely applied in qualitative and quantitative analyses because they are time-consuming sequences [4, 21]. The fast sequences to measure  $T_1$  and  $T_2$ , such as continuous wave free precession (CWFP) and its variant, have more potential for application as industry NMR sensors [6, 8, 9, 11, 12, 20–22]. This technology is described in detail in Sect. 3.1.

For medium- and high-resolution NMR, the time domain signal is too complex to be easily interpreted and must be converted to the frequency domain by Fourier transform [1–4, 6] or other methods, such as filter diagonalization [28]. In these analyses, the NMR signal reflects the chemical environment of the nuclei in the molecules. These properties, known as chemical shift and spin-spin coupling, have been widely employed to determine the structure of pure compounds [1–4]. Moreover, they have also been used in highly selective methods to analyze complex mixtures [6, 28].

## 2.5 NMR Spectrometer

All NMR equipment share the same four basic components (Fig. 3): (i) magnet or static magnetic field  $B_0$  to polarize the spins in the sample; (ii) transmitter to irradiate the specific rf of the nuclear spin transitions; (iii) probe placed in the magnetic field which converts the rf in an oscillating magnetic field  $B_1$  and senses the NMR signal; (iv) receiver which amplifies and detects the NMR signal [1–4].

The electronic hardware of NMR instruments is very well developed and is not a limiting factor for its use in industry. Therefore, as discussed in Sect. 2.2, the magnet is the hardware that restricts the application of NMR in a factory environment. As such, the pros and cons of each type of magnet will be discussed in detail.

Superconducting magnets generate the most intense magnetic fields for NMR. Once energized, the superconducting wire

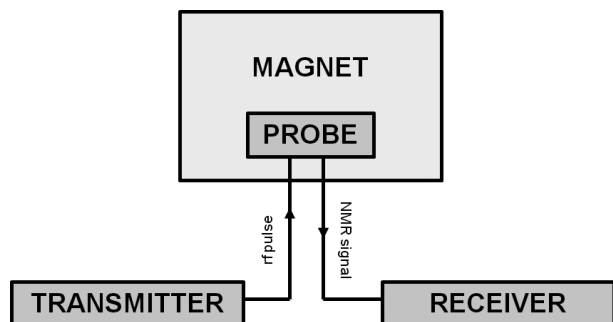


**Figure 3.** Block diagram of basic NMR equipment.

may support high electric currents without any external power source to continuously operate for over ten years, without significant field decays. Accordingly, the fields they produce are also very stable and homogeneous (at least 1 part in  $10^9$ ) and are not perturbed by external sources of interference [1].

Currently, these magnets use wires which only are superconducting at temperatures near the boiling point of liquid helium ( $\sim 4$  K). Thus, these magnets are relatively expensive and require high maintenance costs connected with the consumption of liquid cryogenics (He and  $N_2$ ). They are also bulky because the superconducting coils must be immersed in a Dewar that contains a large volume of liquid helium and is surrounded by a jacket with liquid nitrogen to reduce the radiation onto the He Dewar. The cost and magnet volume limits the application of NMR for industrial sensing. Furthermore, there has been a recent global shortage in the supply of helium which effectively increased its price [29].

While conventional superconducting magnets cooled by liquid cryogenics are currently not a technically or economically feasible option for an industrial NMR sensor, more compact superconducting magnets cooled to low temperature by



**Figure 4.** Cryogen-free desktop 7.05-T NMR magnet (300 MHz for  $^1H$  isotope), with 0.2 ppm resolution and 54 mm room temperature bore [31].

mechanical cryocoolers (Fig. 4) are being tested for NMR applications and seem to be more promising [30, 31].

Resistive electromagnets were employed in high-resolution NMR until the 1970s, but they are no longer in use due to several problems [4]. Namely,  $B_0$  is limited to approximately 2.5 T (100 MHz for  $^1H$ ), they are normally heavier than the permanent magnets, and they need high electric power, most of which is wasted as heat.

Permanent magnets have been used since the introduction of NMR. The maximum commercial NMR magnets are limited to approximately 2.3 T (90 MHz for  $^1H$ ) [32] and were almost abandoned for high-resolution applications since the introduction of superconducting magnets. However, permanent magnets have been the technically and economically feasible option for bench-top low-resolution NMR which has been widely applied in industrial quality control and assurance [6–9, 11, 14–21]. They are also the best option for online NMR sensors and are gaining importance in medium-resolution NMR [6, 32–35].

The strength of permanent magnets depends on the magnetic properties of the ferromagnetic materials and the magnet configuration [6]. There are three classes (but several grades) of ferromagnetic materials used in NMR magnets. While Alnico is the older magnetic material, SmCo and NdFeB (rare earth magnets) represent the new materials in NMR magnets. Tab. 2 summarizes the most important magnetic properties of these materials.  $B_r$  is the remnant field, i.e., the residual magnetization, and is proportional to the magnetic strength.  $T_c$  is the temperature coefficient that indicates the variation of the magnetic field with temperature and  $T_{max}$  is the maximum operational temperature. Consequently, the choice of the material depends on cost (Alnico is cheaper), field strength (NdFeB > SmCo > Alnico), maximum operational temperature, and temperature variation (Alnico > SmCo > NdFeB). Though NdFeB can produce the highest relative magnetic field strength, it has the lowest operational temperature and the greatest sensitivity to temperature variations. Thus, SmCo has been widely applied in NMR due to its temperature drift lower than that of NdFeB.

**Table 2.** Magnetic properties of materials used in NMR magnets.

Material	$B_r$ [T]	$T_c$ [%/°C]	$T_{max}$ [°C]
NdFeB	1.40	−0.12	150
SmCo	1.16	−0.04	300
Alnico	0.07	−0.02	540

$B_r$ : remnant magnetic field;  $T_c$ : temperature coefficient;  $T_{max}$ : maximum operational temperature.

The strength of  $B_0$  also depends on the magnet configuration. The most traditional ways to build permanent NMR magnets are the C or H configurations (Fig. 5). These magnets use two cylinders of magnetic materials assembled in a soft iron box (yoke). The intense and homogeneous magnetic field is produced in the gap between the two magnet poles. However, these magnets are bulky and heavy. The 1.4-T permanent magnets used in 60-MHz spectrometers weigh several hun-

dreds of kilograms and have a volume of approximately  $1 \text{ m}^3$ , even for a 12-cm gap [32].

Halbach solved the weight and volume problems in 1980 by developing a yokeless multipole magnet with oriented rare earth blocks [36]. The magnet blocks are arranged in a cylindrical array, and the minimal Halbach magnets use four magnetic blocks oriented as indicated in Fig. 6a. This design yields the highest field per mass of permanent magnetic material and provides good homogeneity over a large portion of the bore volume [37]. The magnetic field is perpendicular to the cylinder axis to allow the use of sensitive solenoid coils to excite and detect NMR signals (Fig. 6a). They have a very small stray field which does not attract magnetic materials, making them safe and easy to handle and relatively unaffected by metallic objects. Furthermore, they can be opened and closed around the object of interest without a significant force, as demonstrated by Windt et al. (2012) using a simple and elegant Halbach design denoted NMR-CUFF (CUFF denotes cut-open, uniform, force free). Higher-order multipole cylinders have been used to improve  $B_0$  homogeneity [33, 37–40].

The primary advantages of Halbach magnets over the C or H shapes are the reduction of the magnet volume and weight by three orders of magnitude and a large bore/magnet size ratio [37]. Thus, Halbach magnets can be very compact, light, highly homogeneous, and safe and thus make a great option for industrial environments.

Halbach magnets with small and large bores have been built for medium- and low-resolution applications [37]. In 2010, Danieli et al. [37] built a 0.5-kg SmCo Halbach magnet with approximately 0.7 T (30 MHz for  $^1\text{H}$ ) for medium-resolution NMR ( $\sim 0.2$  ppm of the resonance frequency). The magnet is a cylinder with 80 mm length, 35 mm diameter, and 15 mm bore which allows the use of standard 5-mm NMR tubes [33, 37].

Fig. 6b presents a wide-bore (10 cm) low-resolution NMR Halbach 0.23-T ( $\sim 8.7$  MHz for  $^1\text{H}$ ) magnet for applications in oil and food industry [38–40].

Another very important property of the Halbach magnets for industrial applications is the easier construction of very

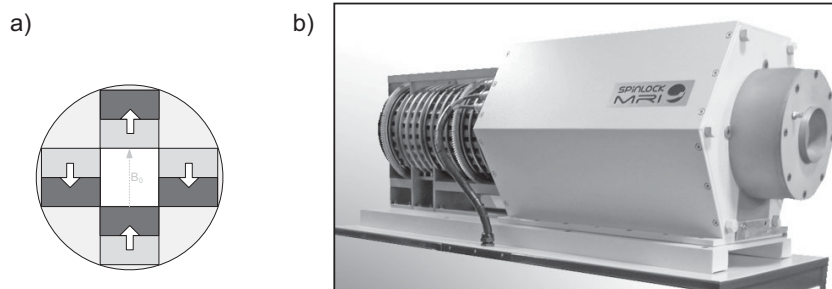


**Figure 6.** (a) Diagram of Halbach magnets with four magnet blocks. (b) Halbach magnet for flow analysis with pre-polarizer magnet [38].

long magnets to pre-polarize the sample for flow analysis. The length of Halbach magnets can be varied by adding or removing Halbach cylindrical arrays. Halbach magnets of several meters in length have been built in recent years for low-resolution NMR industrial applications [38–40]. Therefore, the Halbach magnet is the most important NMR hardware advance in recent years for low- and medium-resolution NMR, and certainly is increasing the likelihood of having, in the near future, a competitive NMR instrument for inline/in situ analysis in industrial environments.

Magnets/probes for remote NMR detection represent another hardware advancement [41–43]. In remote NMR detection, the magnetic field is designed to be outside the magnet. Although this idea is not new [41], the use of new ingenious designs and rare earth materials has increased the number of applications of this concept [42–44]. The major advantage of the remote detection NMR sensor is the almost unlimited size of the sample, in contrast to standard NMR, where the magnet gap or bore limits the sample size [41–44].

Several configurations for remote NMR magnets have been proposed. The most common is the unilateral (or single-side) magnet [42], produced by single or multiple magnetic blocks as demonstrated in Fig. 7. Because these magnets generate magnetic field gradients up to  $10 \text{ Tm}^{-1}$ , several designs have been proposed to reduce these gradients for medium-resolution NMR [44]. In conclusion, the application of low-field permanent magnets is a current technical and economical solution for industrial applications of low- and medium-resolution NMR.

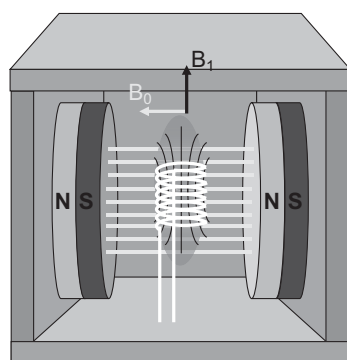


**Figure 5.** Permanent magnet in an H configuration.

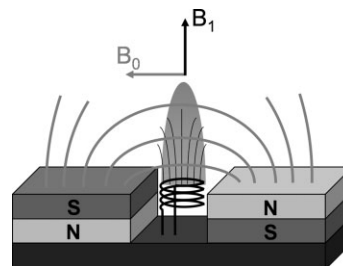


**Figure 7.** Unilateral NMR sensor for remote detection.

### 3 Methods and Instrumental Advances to Enhance S/N

Considering the weakness of NMR signals, sensitivity enhancement is a subject of constant development. Because the intensity of an NMR signal is linearly linked to  $B_0$  (Eq. (4)), attempts at improving the sensitivity of NMR spectroscopy have been focused on magnets with the highest possible  $B_0$  strength [1–3].

In addition to hardware approaches, several methodological approaches have also been implemented to enhance the sensitivity or S/N. Introduced in the late 1960s, the pulsed and FT-NMR and fast signal-averaging protocols were the most significant innovations to enhance S/N [1–4]. Pulsed NMR allowed the fast acquisition of NMR signals, and thus the average of hundreds of NMR signals may be obtained during the time for a single CW scan acquisition. The enhancement of S/N by signal averaging is not linear but depends on the square root of the number of scans ( $n$ ) ( $S/N = n^{1/2}$ ). Thus, a two-fold improvement in S/N requires four-fold NMR scans. This process can be very time-consuming because it is necessary to wait a time of  $5T_1$  between each scan for quantitative analysis using FID or echo signals.

S/N has also been enhanced through instrumental improvements, such as high-quality factor ( $Q$ ) probes, very low-noise amplifiers and digital receivers, as well as several other instrumental advancements [1–3].

In the last two decades, several highly efficient polarization transfer techniques have been proposed to enhance the intensity of NMR signals, such as optical pumping [45], *para*-hydrogen-induced polarization [46], and dynamic nuclear polarization [47–50]. Although these techniques may increase the NMR signal by several orders of magnitude, they are not ideal methods for industrial analyzers because they require the addition of chemical compounds to the sample and sophisticated instrumentation [47–50].

Another important progress in S/N enhancement was the introduction of cryogenic probes (not the sample) which operate at the boiling point of liquid helium [48–50]. These probes significantly improve S/N, but they are expensive and not ideal for industrial sensors.

#### 3.1 Steady-State Free Precession Methods to Enhance S/N

Steady-state free precession (SSFP) sequences have been widely applied in magnetic resonance imaging, high- and low-resolution NMR spectroscopy, or in fast acquisition protocols to enhance S/N by up to two orders of magnitude [9, 20, 21, 51–58]. The major advantage of the SSFP sequences in the enhancement of S/N is that they may be implemented in any pulsed NMR spectrometer without extra hardware or chemical additions to the sample [9, 20, 21].

Carr introduced the SSFP technique to enhance S/N in 1958 [51]. This sequence consists of a train of rf pulses separated by a time interval  $\tau > T_2$  and  $T_1$ . After several pulses, the SSFP regime is attained. It contains an FID-type signal after each pulse

and an echo-type component before the following pulse [9, 20, 21]. Under this regime, the intensity of the NMR signal does not depend on  $T_1$ , and spectra may be acquired during any time interval  $\tau$  [9, 20, 21]. Therefore, a large number of scans per  $T_1$  may be averaged to enhance S/N over conventional pulsed NMR sequences.

SSFP sequences generate the highest improvement in S/N for low-resolution applications [9, 20, 21]. The amplitude signal may be measured using a very short  $\tau$  which is limited by instrumental factors.  $\tau$  as short as 100  $\mu$ s have often been employed, but many experiments were performed with a  $\tau$  of 300  $\mu$ s [9, 20, 21, 53–56] to avoid power amplifier overheating and duty cycle problems. Because  $\tau$  is smaller than  $T_2^*$ , the signal does not decay, and thus this SSFP variant is known as continuous-wave free precession (CWFP) [9, 21]. The FID- and echo-type signals strongly interact in this regime, and the amplitude of the CWFP signal also depends on the precession angle,  $\Psi = \Delta\omega\tau$ , where  $\Delta\omega$  is the offset angular frequency [9, 20]. The signal is maximized when  $\Psi$  is an odd multiple of  $\pi$ ,  $\Psi = (2n+1)\pi$  and is minimal for even multiples,  $\Psi = 2n\pi$ . For  $\Psi = (2n+1)\pi$ , the amplitude of the CWFP signal ( $M_{+,s}$ ) depends on the  $T_1/T_2$  ratio (Eq. (9)). Hence, the amplitude of the CWFP signal when  $T_1 = T_2$  is  $M_0/2$ , decaying to smaller values when  $T_1 > T_2$  [9, 20, 21].

$$M_{+,s} = M_0 T_2 / (T_1 + T_2) \quad (9)$$

Because the CWFP amplitude is constant during the pulse train, it has been employed in high-throughput online methods to measure the oil content of seeds and nuts in a conveyor. Using a 2.1-T wide-bore superconducting magnet, the CWFP method allows the analysis of ten samples per second, with a conveyor velocity of 13  $\text{cm s}^{-1}$  [12].

In addition to sensitivity enhancement, CWFP is neither very sensitive to uncalibrated pulses nor to magnetic field drifts caused by changes in temperature [21]. These are also key features to consider in hostile industrial environments.

According to Litvinov and Dias, NMR relaxation analyses are a valuable tool for real-time monitoring network structure development during cross-linking photopolymerization [59]. In this sense, CWFP sequence may also be a method to monitor fast phase transitions caused by changes in temperature or polymerization reactions [53, 56]. This procedure has been used to measure thermal diffusion in rubber within a few seconds [53] and fast photopolymerization reactions [56]. CWFP was applied to monitor photopolymerization reactions of dimethyl methacrylate blends (dental resins used in restoration) initiated by visible blue light by three photoinitiators: phenylpropanedione (PPD), mono-acylphosphine oxides (MAPO), and canthorquinone (C) [56]. The results of these experiments demonstrate that the photopolymerization reaction was faster for C, followed by PPD and MAPO, and that time constants were approximately 2 s, 10 s, and 20 s, respectively [56].

Another important feature of CWFP sequence that is worth to be highlighted is the use of NMR signals transitioning from thermal equilibrium to the CWFP regime. The signal of this transition has been applied to measure the  $T_1$  and  $T_2$  relaxation times in a single, fast experiment [9, 54]. When a 90°

pulse train equally spaced by  $\tau$  is applied to a system in thermal equilibrium, the resultant signal may be divided into three parts [9, 54]. The first part is characterized by a signal amplitude that alternates between even and odd pulses decaying with a time constant related to  $T_2^*$ . After this oscillatory period, the system enters into the so-called quasi-stationary state (QSS) which decays exponentially to the truly constant regime. When  $\alpha = 90^\circ$  and  $\Psi = (2n+1)\pi$ , the QSS signal decays exponentially with a time constant ( $T^*$ ) depending on both relaxation times given by Eq. (10). The CWFP stationary amplitude is defined by Eq. (9) [9, 54].

$$T^* = 2T_1T_2/(T_1 + T_2) \quad (10)$$

Eqs. (9) and (10) can be rearranged to calculate both relaxation times using the amplitude of the signals after the first pulse ( $\sim M_0$ ), the CWFP regime ( $M_{+,s}$ ), and the time constant  $T^*$ , where  $T_1 = (T^*/2)/(|M_{+,s}|/M_0)$  and  $T_2 = (T^*)/2/[1-(|M_{+,s}|/M_0)]$ . This method was recently used to monitor the  $T_1$  and  $T_2$  relaxation times during the curing process of a single batch of epoxy resin [55].

## 4 Evolution of NMR as Industrial Sensor

Since the discovery of NMR, several articles and patents have demonstrated its potential for flow/inline measurements in factory-like applications [5–9, 23]. The first commercial NMR spectrometer dedicated to the quality control of industrial processes was introduced 40 years ago [6, 9]. It was applied to analyze solid-to-liquid ratios or determine solid fat contents (SFC) [6, 9, 18]. Today, time domain-NMR (TD-NMR) is recognized as a standard international method by several agencies, related to determining the oil and moisture content in seeds and food, the solid fat content of lipids, and the hydrogen content in gasoline [14–19, 39, 50, 60].

Therefore, TD-NMR, medium- and high-resolution NMR have great potential to be incorporated into inline productive processes [5–9, 12, 34, 35, 40, 61, 62]. A short description of some of the works that outline the potential of CW and pulsed NMR in industrial sensors will be presented in the next sections.

### 4.1 Continuous-Wave (CW) Applications

Few years after the discovery of NMR in 1946, Suryan performed the first NMR flow analysis in 1951 [63]. He used a CW- $^1\text{H}$  NMR spectrometer (25 MHz) based on an electromagnet. The experiments were performed with water flowing into an NMR probe through a tube [63]. He observed two significant effects in the NMR signal: an up to 20-fold temporary increase in the signal intensity in comparison to the static sample signal and a subsequent decrease in this signal. He also found that the ratio between the signal amplitudes of the constant flow and static liquids was approximately 5 and dependent on flow speed. From this finding, he concluded that the magnitude of these effects was a function of several factors: the longitudinal relaxation time ( $T_1$ ) of the liquid, the time spent by

the sample inside the magnetic field, the time of permanence inside the rf probe, and the flow velocity [63].

In 1962, Ladner and Stacey used a continuous-flow NMR apparatus to analyze the moisture content in coal [64]. The gravitational flow was maintained at 100 g per hour. Using a  $^1\text{H}$  16-MHz CW spectrometer, it was possible to distinguish the hydrogen signals of the solid material (coal) and the water associated to the coal. The moisture content between 0% and 14% was measured with an accuracy of  $\pm 1\%$ . This experiment was the first application of flow NMR in industrial process control.

After these initial applications, other authors improved the instrumentation and methodologies used in flow measurements. In 1969, McIvor [65] employed a commercial CW equipment with  $B_0 = 1.4\text{ T}$  for the quantitative flow analysis of solvent mixture components with small differences in their chemical shifts. He analyzed samples containing hydrogen and fluorine at 60 and 59.47 MHz, respectively. Furthermore, he was the first to use a serpentine inside the magnet to increase the polarization time such that the spins in the sample were completely polarized before entering the rf probe [65].

Sudmeier and Pesek (1971) published the first CW-NMR study using a stop-and-flow method [66]. The authors monitored the line width of  $^{35}\text{Cl}$  NMR as a function of time after mixing Hg and bovine serum albumin with various chelating agents in a study of an important model of chelating therapy.

After these publications, the application of CW-NMR to flowing samples nearly ended due to the popularization of pulsed NMR spectrometers. However, Hills and Wright developed a new version of a CW-NMR equipment for flow measurements in 2006 [5]. They proved that the sample's translation in flow could be used to detect NMR signals without an excitation pulse or gradient field application. When the samples passing through the sensor (probe) were excited by  $B_1$ , they generated an NMR signal that was employed in the measurements.

### 4.2 Pulsed NMR Applications

Singer reported the first application of pulsed-flow NMR in 1959, when he studied blood flow in rat tails [67]. He measured the longitudinal relaxation time of the hydrogen atoms belonging to the water in blood and the change in  $T_1$  as a function of blood flow interruption with a tourniquet. Because the flow reduced the saturation of the water signal, an increase in the signal intensity with blood flow was found.

In 1971, Grover and Singer developed the first medical application of flow NMR by measuring the blood flow velocity inside a human finger using spin-echo sequences [68]. Because the echo intensity depends on flow, it was possible to determine the velocity distribution of blood.

In 1978, Watanabe and Niki introduced a coupled HR-NMR and HPLC technique by means of a  $^1\text{H}$  60-MHz pulsed spectrometer and the stop-and-flow method [69]. Many authors subsequently proposed analyses with chromatographic eluents in continuous flow via high-field superconductor magnets with increased NMR sensitivity. Special devices have been developed to interface NMR with chromatography to polarize

the sample [70]. HPLC-NMR systems are becoming commonplace in research labs to isolate, detect, quantify, and/or identify compounds primarily in the analysis of natural products, drug purification, and metabolites of biological fluids [71].

The first demonstration of flow measurements by a train of equidistant rf pulses in the presence of a static field gradient was done by Hemminga and Jager in 1980 [72], the so-called repetitive pulse method, which is, in essence, identical to CWFP. Such method has been used to measure flow in plants in 1984 [73]. Also a portable NMR was developed based on the principles of the repetitive pulse method [74].

Pearson et al. (1987) described a pulsed method to analyze wheat moisture content by a CPMG sequence [75]. In the same year, Renou et al. demonstrated that TD-NMR pulsed techniques can simultaneously determine the ethanol and sugar content using low-field NMR [76].

In 1991, Nicholls and De Los Santos developed a  $^1\text{H}$  11-MHz spectrometer NMR sensor to measure the moisture content in the wet milling corn industry [77]. The sensor was developed when a U.S. government study showed that the drying process in this industry was consuming approximately 8% of all the industrial energy used in the USA. In this system, the wet corn was carried by a gutter to the NMR sensor that was filled with a sample pressed by a piston. After signal acquisition, the piston returned the sample to the process. In this work, correlation to the moisture sample was performed by  $T_1$  and  $T_2$  relaxation times.

In 1993, Chen et al. developed an online 2.1-T NMR sensor to evaluate ripening in intact avocados via FT-NMR, TD-NMR, and MRI techniques [78]. They observed good correlation between the ripening stage of the avocados and the NMR measurements. Zion et al. in 1997 used the same online 2.1-T NMR/MRI equipment to classify olives with and without pits [79]. They analyzed the olives moving up to  $25\text{ cm s}^{-1}$ . The classification errors were 4.3, 4.7, 2.3, and 4.0% for conveyor speeds of 0, 5, 15, and  $25\text{ cm s}^{-1}$ , respectively.

In 2001, Azeredo et al. studied the effect of flow on the CWFP signal [11]. Using a  $^1\text{H}$  7.5-MHz home-made spectrometer, they proved the dependence of the water CWFP signal on the speed, flow direction, magnetic field gradient,  $T_1$  and  $T_2$  relaxation times, and refocusing angle.

Corver et al. in 2005 demonstrated an inline non-contact check weigher (NCCW) method using the TD-NMR technology. NMR can offer a fast and simple (one-step) alternative to weighing by a balance, without the need for the sample to be removed from the vial [80].

In 2007, Colnago et al. used a CWFP signal to measure the oil content of seeds in a conveyor traveling at  $13\text{ cm s}^{-1}$  [12] and demonstrated that the CWFP sequence enabled to measure up to ten samples per second.

In 2007, Hernandez-Sanchez et al. evaluated the internal browning of pears using online TD-NMR and MRI equipment [81]. The images of the pears moving at  $54\text{ mm s}^{-1}$  allowed normal pears to be distinguished from pears with internal browning.

Also in 2007, Prestes et al. used the CPMG sequence in stop-and-flow equipment mode to measure the oil quality of more than 1000 intact seeds per hour with a 2.1-T superconductor

magnet [23]. They observed that CPMG decay strongly correlates with oil quality in food and biodiesel applications.

In 2009, Corrêa et al. used the CWFP signal, which depends on  $T_1$  and  $T_2$ , to determine the intramuscular fat content in beef with the stop-and-flow mode [22]. The CWFP signal showed a higher correlation ( $r = 0.9$ ) with the intramuscular fat contents than the one obtained with the CPMG signal ( $r = 0.25$ ), which depends only on  $T_2$  [22].

In 2011, Colnago et al. measured the oil quality of seeds by CWFP using the stop-and-flow mode [9]. The  $T_2$  values obtained by CWFP strongly correlated ( $r > 0.90$ ) with those obtained by CPMG, indicating that CWFP was suitable to measure oil quality.

In 2011, Andrade et al. applied a CPMG sequence with refocusing flip angles lower than  $180^\circ$  to reduce overload problems when NMR equipment is used in flow analyses [24]. By means of  $90^\circ$  refocusing flip angles, the rf power was reduced by 25% with respect to the conventional CPMG sequence.

In 2011, Osán et al. proposed a rapid method to measure the average velocities of turbulent flows using CPMG sequences [40]. The application of this method in a spectrometer with a 0.255-T magnet and pre-polarization stacks on both sides of the rf section allowed the bidirectional measurement of oil, water, and gas moving at speeds up to  $2.7\text{ m s}^{-1}$  in a petroleum pipe, with a cylindrical region of interest (ROI) of 10 cm diameter and 10 cm length [37–39, 82]. The prototype meter was tested with water-oil, water-gas, and oil-water-gas mixtures [82]. In addition to measuring the flow velocity and fluid fractions, the implementation of a three-coil gradient system set enabled the acquisition of 2D magnetic resonance images and velocity profiles of the ROI cross section, with a spatial imaging resolution of approximately 1 cm [82].

Andrade et al. (2012) developed a new method to measure online the oilseed quality using a Carr-Purcell (CP) sequence with  $90^\circ$  refocusing flip angles. This method was named CP-CWFP because it depends on  $T_1$  and  $T_2$ , much like CWFP [83]. The CP-CWFP sequence is more efficient than CWFP to measure the relaxation time when  $T_1 \sim T_2$ , a situation normally observed in low-field NMR.

## 5 Perspectives and Conclusions

Referring back to the question addressed in the title, it is a consensus that there are still some challenges ahead before inline NMR can be disseminated as sensor in factories, such as: (i) the inherent low sensitivity, (ii) the need of a magnetic field, (iii) the time required for sample polarization, and (iv) the implementation cost. However, fast developments on NMR in order to overcome these bottlenecks enable to envisage this technology playing a larger role in industrial applications for the next decade.

Among the potential techniques that may increase the applications of NMR in the industrial sector, adiabatic pulses [84, 85], ultrafast 2D NMR [86, 87], fast droplet sizing distribution (DSD) measurements [88, 89], and reaction monitoring in medium-resolution NMR spectroscopy [6, 25] can be highlighted.

Adiabatic pulses are becoming popular in HR-NMR and MRI [84, 85]. This method combines the advantages of CW and pulsed NMR in a single experiment and can be applied to acquire signals during excitation or a few microseconds after the pulse. This feature is very important to measure the signals of solid components with very short  $T_2$  or  $T_2^*$ . In MRI, this method has been used to analyze the solid component of animal and human tissues, such as teeth and bones [84].

Ultrafast 2D NMR has been a powerful technique to enhance the selectivity of high-resolution spectra in a fraction of a second [86, 87]. Despite its demonstrated applicability in HR-NMR, ultrafast 2D NMR can potentially be applied to medium-resolution NMR for rapid chemical and physical analyses of complex mixtures and reactions in the manufacturing sector.

Droplet sizing distribution (DSD) analysis is a well-established NMR-PFG technique [90], but the long acquisition time is one critical issue that limits its use in inline industrial applications. However, the development of faster diffusion measurement techniques [91] can certainly contribute to this area.

Finally, according to a very recent review [6], medium-resolution (MR) NMR spectroscopy is currently a fast developing field which has an enormous potential to monitor the physico-chemical properties of complex feedstock mixtures and reactions in real time. As a good example of this potential, coupling between NMR and size-exclusion chromatography (SEC) to produce an online SEC-NMR spectrum by a benchtop low-field NMR instrument can be emphasized, as demonstrated for polymer analyzes by Cudaj et al. (2012) [92].

Although several papers and patents have been described that indicate the potential of NMR as an industrial sensor, we believe that one or more NMR companies will soon be offering a general-purpose, cost-effective NMR sensor for the manufacturing sector. Some of these companies include (in alphabetic order): Acquitex [93], Agilent [48], Anasazi [32], Bruker [50], CEM [94], Cryogenic [31], HTS-110 [30], Jeol [95], Magritek [33], Modcon [96], Nanalysis [97], Niumag [98], One Resonance Sensor [99], Oxford [60], Process NMR Associates [100], Qualion NMR [101], Resonance Systems [102], SpinCore [103], Spinlock [39], Stelar [104], Tecmag [105], Thermo Scientific [106], UNIQ PMR [107], and Xigo Nanotools [108].

Given the potential of NMR, new technologies available and the number of companies working on the field, we believe that NMR will soon be widely used as inline industrial sensor to precisely control and automate processes in an unprecedented manner.

## Acknowledgment

We wish to thank FAPESP and CNPq (Brazilian agencies) for financial support. L. M. C., T. M. O., and D. J. P. are also grateful to CONICET for financial assistance.

*The authors have declared no conflict of interest.*

## References

- [1] M. H. Levitt, *Spin Dynamics: Basic of Nuclear Magnetic Resonance*, 2nd ed., John Wiley and Sons, Chichester **2009**.
- [2] A. Abragam, *The Principle of Nuclear Magnetism*, Clarendon Press, **1978**.
- [3] R. R. Ernst, G. Bodenhausen, A. Wokaun, *Principles of Nuclear Magnetic Resonance in one and two Dimensions*, Clarendon Press, Oxford **1990**.
- [4] T. C. Farrar, E. D. Becker, *Pulse and Fourier Transform NMR: Introduction to Theory and Methods*, Academic Press, New York **1971**.
- [5] B. P. Hills, K. M. Wright, *J. Magn. Reson.* **2006**, *178* (2), 193–205. DOI: 10.1016/jmr.2005.09.010
- [6] F. Dalitz, M. Cudaj, M. Maiwald, G. Guthausen, *Prog. Nucl. Magn. Reson. Spectrosc.* **2012**, *60* (1), 52–70. DOI: 10.1016/j.pnmr.2011.11.003
- [7] E. Frauendorfer, A. Wolf, W. Hergeth, *Chem. Eng. Technol.* **2010**, *33* (11), 1767–1778. DOI: 10.1002/ceat.201000265
- [8] J. Van Duynhoven, A. Voda, M. Witek, H. van As, *Annu. Rep. NMR Spectrosc.* **2010**, *69* (1), 145–197. DOI: 10.1016/S0066-4103(10)69003-5
- [9] L. A. Colnago, R. B. V. Azeredo, A. Marchi Netto, F. D. Andrade, T. Venâncio, *Magn. Reson. Chem.* **2011**, *49* (SI), S113–S120. DOI: 10.1002/mrc.2841
- [10] R. K. Harris, E. D. Becker, S. M. C. De Menezes, R. Goodfellow, P. Granger, *Pure Appl. Chem.* **2001**, *73* (11), 1795–1818. DOI: 10.1351/pac200173111795
- [11] R. B. D. Azeredo, M. Engelsberg, L. A. Colnago, *Phys. Rev. E* **2001**, *64* (1), 16309–16313. DOI: 10.1103/PhysRevE.64.016309
- [12] L. A. Colnago, M. Engelsberg, A. A. Souza, L. L. Barbosa, *Anal. Chem.* **2007**, *79* (3), 1271–1274. DOI: 10.1021/ac062091+
- [13] R. K. Gupta, J. A. Ferretti, E. D. Becker, *J. Magn. Reson.* **1974**, *13* (3), 275–290. DOI: 10.1016/0022.2364(74)90022-5
- [14] *IUPAC Norm Version 2150, Solid content determination in fats by NMR – Low resolution nuclear magnetic resonance*, Blackwell Scientific Publication, Oxford **1987**.
- [15] ISO 10565, *Oilseeds – Simultaneous determination of oil and water contents – Method using pulsed nuclear magnetic resonance spectrometry*, International Organization for Standardization, Geneva **1998**.
- [16] ISO 8292, *Animal and vegetable fats and oils – Determination of solid fat content – Pulsed nuclear magnetic resonance method*, International Organization for Standardization, Geneva **1991**.
- [17] ISO 10632, *Oilseed residues – Simultaneous determination of oil and water contents – Method using pulsed nuclear magnetic resonance spectroscopy*, International Organization for Standardization, Geneva **2000**.
- [18] *AOCS Official Method Cd 16b*, American Oil Chemist Society, Urbana, IL **1993**.
- [19] *AOCS Method Ak 4-02*, American Oil Chemist Society, Urbana, IL **1995**.
- [20] R. B. D. Azeredo, L. A. Colnago, M. Engelsberg, *Anal. Chem.* **2000**, *72* (11), 2401–2405. DOI: 10.1021/ac991258e

- [21] R. B. V. Azeredo, L. A. Colnago, A. A. Souza, M. Engelsberg, *Anal. Chim. Acta* **2003**, *478* (2), 313–320. DOI: 10.1016/S0003-2670(02)01514-3
- [22] C. C. Correa, L. A. Forato, L. A. Colnago, *Anal. Bioanal. Chem.* **2009**, *393* (4), 1357–1360. DOI: 10.1007/s00216-008-2526-6
- [23] R. A. Prestes, L. A. Colnago, L. A. Forato, E. Carrilho, R. B. Bassanezi, N. A. Wulff, *Mol. Plant Pathol.* **2009**, *10* (1), 51–57. DOI: 10.1016/j.aca.2007.06.022
- [24] F. D. de Andrade, A. M. Netto, L. A. Colnago, *Talanta* **2011**, *84* (1), 84–88. DOI: 10.1016/j.talanta.2010.12.033
- [25] F. Mariette, *Curr. Opin. Colloid Interface Sci.* **2009**, *14* (3), 203–211. DOI: 10.1016/j.cocis.2008.10.006
- [26] F. M. Verbi Pereira, L. A. Colnago, *Food Anal. Methods* **2012**, *5* (6), 1349–1353. DOI: 10.1007/s12161-012-9383-9
- [27] F. M. Verbi Pereira, A. Carvalho, L. F. Cabeça, L. A. Colnago, *Microchem. J.* **2013**, *108* (1), 14–17. DOI: 10.1016/j.microc.2012.12.003
- [28] R. M. Maria, T. B. Moraes, C. J. Magon, T. Venâncio, W. F. Altei, A. D. Andricopulo, L. A. Colnago, *Analyst* **2012**, *137* (19), 4546–4551. DOI: 10.1039/c2an35451a
- [29] M. S. Reisch, *Chem. Eng. News* **2012**, *90* (29), 32–34. DOI: 10.1021/cen-09029-bus3
- [30] *HTS-110*, <http://hts100.co.nz/nmr/> (accessed: May 2013).
- [31] *Cryogenic*, [www.cryogenic.co.uk](http://www.cryogenic.co.uk) (accessed: May 2013).
- [32] *Anasazi-Instruments, No Cryogen NMR*, [www.aliinmr.com/EM\\_Magnet\\_Upgrades.html](http://www.aliinmr.com/EM_Magnet_Upgrades.html) (accessed: May 2013).
- [33] *Innovative NMR and MRI Solutions*, [www.magritek.com/](http://www.magritek.com/) (accessed: May 2013).
- [34] M. A. Vargas, M. Cudaj, K. Hailu, K. Sachsenheimer, G. Guthausen, *Macromolecules* **2010**, *43* (13), 5561–5568. DOI: 10.1021/ma1006599
- [35] A. Nordon, A. Diez-Lazaro, C. W. L. Wong, C. A. McGill, D. Littlejohn, M. Weerasinghe, D. A. Mammam, M. L. Hitchman, J. Wilkie, *Analyst* **2008**, *133* (3), 339–347. DOI: 10.1039/b714266h
- [36] K. Halbach, *Nucl. Instrum. Methods* **1980**, *169* (1), 1–10. DOI: 10.1016/0029-554X(80)90094-4
- [37] E. Danieli, J. Perlo, B. Blümich, F. Casanova, *Angew. Chem., Int. Ed.* **2010**, *49* (24), 4133–4135. DOI: 10.1002/anie.201000221
- [38] D. Pusiol, M. Carpinella, G. Albert, T. Osán, J. M. Ollé, J. J. Freeman, M. Appel, I. S. Lopez Gamundi Espejo, *US Patent 7 872 474 B2*, **2011**.
- [39] *Spinlock, Magnetic Resonance Solutions*, <http://nmr-spectrometers.com> (accessed: May 2013).
- [40] T. M. Osán, J. M. Olle, M. Carpinella, L. M. C. Cerioni, D. J. Pusiol, M. Appel, J. Freeman, I. Espejo, *J. Magn. Reson.* **2011**, *209* (2), 116–122. DOI: 10.1016/j.jmr.2010.07.011
- [41] J. A. Jackson, L. J. Burnett, J. F. Harmon, *J. Magn. Reson.* **1980**, *41* (3), 411–421. DOI: 10.1016/0022-2364(80)90298-X
- [42] E. Danieli, B. Blümich, *J. Magn. Reson.* **2013**, *229* (1), 142–154. DOI: 10.1016/j.jmr.2012.11.023
- [43] L. F. Cabeça, L. V. Marconcini, G. P. Mambrini, R. B. V. Azeredo, L. A. Colnago, *Energy Fuels* **2011**, *25* (6), 2696–2701. DOI: 10.1021/ef200294j
- [44] J. Perlo, F. Casanova, B. Blümich, *J. Magn. Reson.* **2006**, *180* (2), 274–279. DOI: 10.1016/j.jmr.2006.03.004
- [45] R. Tycko, S. E. Barrett, G. Dabbagh, L. N. Pfeiffer, K. W. West, *Science* **1995**, *268* (5216), 1460–1463. DOI: 10.1126/science.7539550
- [46] S. B. Duckett, R. E. Mewis, *Acc. Chem. Res.* **2012**, *45* (8), 1247–1257. DOI: 10.1021/ar2003094
- [47] J. H. Ardenkjaer-Larsen, B. Fridlund, A. Gram, G. Hansson, L. Hansson, M. H. Lerche, R. Servin, M. Thaning, K. Golman, *Proc. Natl. Acad. Sci. U.S.A.* **2003**, *100* (18), 10158–10163. DOI: 10.1073/pnas.1733835100
- [48] *Agilent*, [www.chem.agilent.com](http://www.chem.agilent.com) (accessed: May 2013).
- [49] P. L. de Sousa, R. E. de Souza, M. Engelsberg, L. A. Colnago, *J. Magn. Reson.* **1998**, *135* (1), 118–125. DOI: 10.1006/jmre.1998.1559
- [50] *Innovation with Integrity*, [www.bruker.com](http://www.bruker.com) (accessed: May 2013).
- [51] H. Y. Carr, *Phys. Rev.* **1958**, *112* (5), 1693–1701. DOI: 10.1103/PhysRev.112.1693
- [52] O. Bieri, K. Scheffler, *J. Magn. Reson. Imaging* **2013**, *38* (1), 2–11. DOI: 10.1002/jmri.24163
- [53] T. Venâncio, M. Engelsberg, R. B. V. Azeredo, N. E. R. Alem, L. A. Colnago, *J. Magn. Reson.* **2005**, *173* (1), 34–39. DOI: 10.1016/j.jmr.2004.11.01
- [54] T. Venâncio, M. Engelsberg, R. B. V. Azeredo, L. A. Colnago, *J. Magn. Reson.* **2006**, *181* (1), 29–34. DOI: 10.1016/j.jmr.2006.03.011
- [55] T. Venâncio, L. A. Colnago, *Magn. Reson. Chem.* **2012**, *50* (8), 534–538. DOI: 10.1002/mrc.3834
- [56] L. A. Colnago, R. B. V. Azeredo, I. Coelho, M. I. B. Tavares, M. Engelsberg, *Ann. Magn. Reson.* **2003**, *2* (3), 125–127.
- [57] R. R. Ernst, W. A. Anderson, *Rev. Sci. Instrum.* **1966**, *37* (1), 93–102. DOI: 10.1063/1.1719961
- [58] P. M. dos Santos, A. A. de Souza, L. A. Colnago, *Appl. Magn. Reson.* **2011**, *40* (3), 331–338. DOI: 10.1007/s00723-011-0209-5
- [59] V. M. Litvinov, A. A. Dias, *Macromol. Symp.* **2005**, *230* (1), 20–25. DOI: 10.1002/masy.200551137
- [60] *The Business of Science*, [www.oxford-instruments.com/industries-and-applications/research/nmr](http://www.oxford-instruments.com/industries-and-applications/research/nmr) (accessed: May 2013).
- [61] C. Tellier, F. Mariette, *Annu. Rep. NMR Spectrosc.* **1995**, *31* (1), 105–122. DOI: 10.1016/S0066-4103(08)60145-3
- [62] F. D. de Andrade, L. A. Colnago, *Quim. Nova* **2012**, *35* (10), 2019–2024. DOI: 10.1590/S0100-40422012001000023
- [63] G. Suryan, *Proc. Indian Acad. Sci., Sec. A* **1951**, *33* (1), 107–111. DOI: 10.1007/BF03172192
- [64] W. R. Ladner, A. E. Stacey, *Br. J. Appl. Phys.* **1962**, *13* (3), 136. DOI: 10.1088/0508-3443/13/3/118
- [65] M. C. McIvor, *J. Phys., E* **1969**, *2* (3), 292–293. DOI: 10.1088/0022-3735/2/3/421
- [66] J. L. Sudmeier, J. J. Pesek, *Inorg. Chem.* **1971**, *10* (4), 860–863. DOI: 10.1021/ic50098a040
- [67] J. R. Singer, *Science* **1959**, *130* (3389), 1652–1653. DOI: 10.1126/science.130.3389.1652
- [68] T. Grover, J. R. Singer, *J. Appl. Phys.* **1971**, *42* (3), 938–940. DOI: 10.1063/1.1660189
- [69] N. Watanabe, E. Niki, *Proc. Jpn. Acad., Ser. B* **1978**, *54* (4), 194–199. DOI: 10.2183/pjab.54.194
- [70] J. F. Haw, T. E. Glass, D. W. Hausler, E. Motell, H. C. Dorn, *Anal. Chem.* **1980**, *52* (7), 1135–1140. DOI: 10.1021/ac50057a32

- [71] J. C. Lindon, J. K. Nicholson, I. D. Wilson, *J. Chromatogr., B* **2000**, 748 (1), 233–258. DOI: 10.1016/S0378-4347(00)00320-0
- [72] M. A. Hemminga, P. A. DeJager, *J. Magn. Reson.* **1980**, 37 (1), 1–16. DOI: 10.1016/0022-2364(80)90088-8
- [73] H. van As, T. J. Schaafsma, *Biophys. J.* **1984**, 45 (2), 469–472. DOI: 10.1016/S0006-3495(84)84170-3
- [74] H. van As, J. E. A. Reinders, P. A. DeJager, P. Vandesanden, T. J. Schaafsma, *J. Exp. Bot.* **1994**, 45 (270), 61–67. DOI: 10.1093/jxb/45.1.61
- [75] R. M. Pearson, L. R. Ream, C. Job, J. Adams, *Cereal Foods World* **1987**, 32 (11), 822–826.
- [76] J. P. Renou, A. Briguet, P. Gatellier, J. Kopp, *Int. J. Food Sci. Technol.* **1987**, 22 (2), 169–172. DOI: 10.1111/j.1365-2621.1987.tb00473.x
- [77] C. I. Nicholls, A. D. Santos, *Drying Technol.* **1991**, 9 (4), 849–873. DOI: 10.1080/07373939108916724
- [78] P. Chen, M. J. McCarthy, R. Kauten, Y. Sarig, S. Han, *J. Agric. Eng. Res.* **1993**, 55 (3), 177–187. DOI: 10.1006/jaer.1993.1042
- [79] B. Zion, S. M. Kim, M. J. McCarthy, P. Chen, *J. Sci. Food Agric.* **1997**, 75 (4), 496–502. DOI: 10.1002/(SICI)1097-0010(199712)
- [80] J. Corver, G. Guthausen, A. Kamlowski, *Pharm. Eng.* **2005**, 25 (3), 18–30.
- [81] N. Hernandez-Sanchez, B. P. Hills, P. Barreiro, N. Marigheito, *Postharvest Biol. Technol.* **2007**, 44 (3), 260–270. DOI: 10.1016/j.postharvbio.2007.01.002
- [82] M. Appel, J. J. Freeman, D. Pusiol, *SPE Middle East Oil and Gas Show and Conference*, Manama, BH, September **2011**.
- [83] F. D. de Andrade, A. M. Netto, L. A. Colnago, *J. Magn. Reson.* **2012**, 214 (1), 184–188. DOI: 10.1016/j.jmr.2011.11.004
- [84] D. Idiyatullin, S. Suddarth, C. A. Corum, G. Adrian, M. Garwood, *J. Magn. Reson.* **2012**, 220 (1), 26–31. DOI: 10.1016/j.jmr.2012.04.016
- [85] M. Garwood, L. DelaBarre, *J. Magn. Reson.* **2001**, 153 (2), 155–177. DOI: 10.1006/jmre.2001.2340
- [86] K. J. Donovan, E. Kupce, L. Frydman, *Angew. Chem., Int. Ed.* **2013**, 52 (15), 4152–4155. DOI: 10.1002/anie.201210070
- [87] L. H. K. Queiroz Jr., D. P. K. Queiroz, L. Dhooghe, A. G. Ferreira, P. Giraudeau, *Analyst* **2012**, 137 (10), 2357–2361. DOI: 10.1039/C2AN16208C
- [88] K. G. Hollingsworth, A. J. Sederman, C. Buckley, L. F. Gladden, M. L. Johns, *J. Colloid Interface Sci.* **2004**, 274 (1), 244–250. DOI: 10.1016/j.jcis.2004.02.074
- [89] J. P. M. van Duynhoven, B. Maillet, J. Schell, M. Tronquet, G.-J. W. Goudappel, E. Trezza, A. Bulbarelo, D. van Dusschoten, *Eur. J. Lipid Sci. Technol.* **2007**, 109 (11), 1095–1103. DOI: 10.1002/ejlt.200700019
- [90] M. L. Johns, *Curr. Opin. Colloid Interface Sci.* **2009**, 14 (3), 178–183. DOI: 10.1016/j.cocis.2008.10.005
- [91] J. Mitchell, M. L. Johns, *Concepts Magn. Reson., Part A* **2009**, 34A (1), 1–15. DOI: 10.1002/cmra.20128
- [92] M. Cudaj, G. Guthausen, T. Hofe, M. Wilhelm, *Macromol. Chem. Phys.* **2012**, 213 (18), 1933–1943. DOI: 10.1002/macp.201200290
- [93] *Acquitek*, [www.acquitek.com/nmr-processor/rf-acquisition-excitation-system.html](http://www.acquitek.com/nmr-processor/rf-acquisition-excitation-system.html) (accessed: May 2013).
- [94] *CEM*, [www.cem.com/fast-trac.html](http://www.cem.com/fast-trac.html) (accessed: May 2013).
- [95] *Jeol*, [www.jeol.co.jp/](http://www.jeol.co.jp/) (accessed: May 2013).
- [96] *Modcon*, [www.modcon-systems.com/](http://www.modcon-systems.com/) (accessed: May 2013).
- [97] *Nanalysis*, [www.nanalysis.com/](http://www.nanalysis.com/) (accessed: May 2013).
- [98] *Niumag*, [http://en.niumag.com/detail\\_product.php?id=324](http://en.niumag.com/detail_product.php?id=324) (accessed: May 2013).
- [99] *One Resonance Sensor*, <http://detect-ors.com/> (accessed: May 2013).
- [100] *PNA, Process NMR Associates*, [www.process-nmr.com/](http://www.process-nmr.com/) (accessed: May 2013).
- [101] *Qualion, NMR Analyzers*, <http://qualion-nmr.com/> (accessed: May 2013).
- [102] *Resonance System*, [www.nmr-design.com](http://www.nmr-design.com) (accessed: May 2013).
- [103] *SpinCore Technologies, Inc.*, [www.spincore.com/](http://www.spincore.com/) (accessed: May 2013).
- [104] *Stelar*, [www.stelar.it/](http://www.stelar.it/) (accessed: May 2013).
- [105] *Tecmag*, <http://tecmag.com/> (accessed: May 2013).
- [106] *Thermo Scientific*, [www.picospin.com/products/picospin-45/](http://www.picospin.com/products/picospin-45/) (accessed: May 2013).
- [107] *UNIQ PMR*, [www.mrr.com/pdf/UNIQ-PMR\\_sm.pdf](http://www.mrr.com/pdf/UNIQ-PMR_sm.pdf) (accessed: May 2013).
- [108] *Xigo Nanotools*, [www.xigonanotools.com](http://www.xigonanotools.com) (accessed: May 2013).